



A systematic investigation of current efficiency during brass deposition from a pyrophosphate electrolyte using RDE, RCE, and QCM

K. Johannsen^a, D. Page^b, S. Roy^{b,*}

^a Department of Chemistry, University of Aarhus, Langelandsgade, 8000 Aarhus, Denmark

^b Department of Chemical and Process Engineering, University of Newcastle, Newcastle, NE1 7RU, UK

Received 1 September 1999; received in revised form 6 December 2000

Abstract

The pyrophosphate electrolyte has been used for brass deposition as a replacement for cyanide electrolytes. However, there is considerable confusion about the current efficiency of brass deposition from this electrolyte. This study uses a rotating disc electrode (RDE), a rotating cylinder electrode (RCE) and a quartz crystal microbalance (QCM) to systematically determine the current efficiency of copper, zinc, and brass deposition from a pyrophosphate electrolyte. Electrodeposition of brass on RCE and QCM show that the current efficiency for copper, zinc as well as brass is well below 100%. Simultaneous measurement of current and frequency at a QCM showed that pyrophosphate is adsorbed at the electrode surface during copper reduction. However, when zinc is present in the solution, pyrophosphate adsorption is blocked. © 2000 Elsevier Science Ltd. All rights reserved.

Keywords: Electrochemical quartz crystal microbalance; Electrodeposition; Pyrophosphate; Copper; Zinc; Alloy deposition

1. Introduction

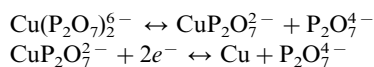
Brass has been electrodeposited mainly for decorative purposes or for corrosion protection. Much of the earlier work as well as many industrial processes have focused on electrodeposition from a cyanide electrolyte, mainly because brass is deposited from cyanides at high current efficiency (> 75%) and it has a smooth and bright texture [1,2]. Alternative complexing agents such as citrate, thiocyanate, tartrate and pyrophosphate [1–3] have been sought in recent years because cyanide processes pose environmental and safety hazards. The most promising electrolyte that has received attention from several research groups, is a pyrophosphate-based complexing solution [3–7].

Although the earliest suggestion of feasibility of Cu–Zn deposition from pyrophosphate electrolytes was proposed in 1912 [4], the first systematic data on metal deposition from this electrolyte was gathered by Rama Char and co-workers in 1956 [3,5–7]. Their research showed that copper, nickel, zinc and tin or an alloy of these metals can be electrodeposited from pyrophosphate electrolytes. They suggested that, in order to plate brass, an electrolyte containing a low ionic concentration of copper and a high ionic concentration of zinc should be used. The metal to pyrophosphate ion ratio should be 2.2. An excess of potassium pyrophosphate is necessary as supporting electrolyte as well as to maintain the bath pH at ≈ 8.5 . At this pH the electrolyte is stable (does not precipitate) [6,7] and the bath is buffered. They found that sound deposits were obtained at electrolyte temperatures between 40–80°C and that the current efficiency of metal deposition was close to 100% [6,7].

* Corresponding author. Tel.: +44-191-2227274; fax: +44-191-2225292.

More recent empirical investigations on copper and zinc electrodeposition from pyrophosphate electrolytes, however, have raised questions regarding the current efficiency results of Rama Char and co-workers. For example, Cu–Ni deposition from a pyrophosphate solution showed that current efficiencies can be as low as 50% when alloys containing up to 50% Ni were plated [8]. High current efficiencies were obtained only when the copper content in the electrolyte was high. In a subsequent study, the same researchers reported that the current efficiency for copper deposition from a pyrophosphate solution was as low as 50% and that for Cu–Ni alloy deposition was about 20% [9]. A separate study also indicated that electrodeposition of Cu–Zn alloys from pyrophosphate electrolytes exhibits a low current efficiency when the deposition current is high [10]; no systematic data on current efficiency, however, was provided in that work. No information on side reactions has been provided in these studies.

In the absence of adequate systematic data on brass deposition from pyrophosphate solutions, some insight can be gleaned from individual copper or zinc reduction studies. Konno and Nagayama [12] have studied copper reduction from electrolytes containing copper and potassium pyrophosphate. In their work, Cu(II) concentration was either 0.1 or 0.5 M and the ratio of copper to pyrophosphate ranged between 2 and 5. They found that the reversible potential for copper shifted to more negative values when the concentration of pyrophosphate was increased. In addition, two different Tafel slopes were obtained for copper reduction; the change in slope occurred at -0.75 V versus SCE. They proposed that copper was reduced from $[\text{Cu}(\text{P}_2\text{O}_7)_2]^{6-}$ complex and that the deposition mechanism was dependent on the pyrophosphate concentration. The electrochemical reactions for copper reduction are:



Copper is reduced directly from $[\text{Cu}(\text{P}_2\text{O}_7)_2]^{6-}$ when the concentration of $(\text{P}_2\text{O}_7)^{4-}$ in the solution is high. They showed that pyrophosphate is adsorbed on the surface at -0.75 V versus SCE where smooth copper deposits were obtained [12,13]. They stated that the current efficiency for copper deposition was 100%, although the procedure used for current efficiency measurements was not reported.

Electrodeposition of zinc and brass from a pyrophosphate electrolyte was carried out by Vagramyan et al. [14]. They encountered several problems: (1) a significant amount of oxygen ($> 28\%$ atomic) was deposited with zinc and brass, thereby bringing into question whether the deposits were metallic, (2) most deposits were cracked and therefore not useful, (3) metallic deposits contained only a low atomic content of zinc.

In fact, their experimental results showed that pyrophosphate was inappropriate for brass electrodeposition. In addition, it is recognised that oxide and hydroxides are deposited when there is significant hydrogen evolution (leading to changes in surface pH), that means current efficiency for zinc and brass deposition was low. Copper and zinc deposition investigations show that there is a gap in the current efficiency results — although hydrogen evolution is low during copper deposition, it is significant when zinc is reduced from the same solution.

Additional insight to Cu–Zn co-deposition can be gained from the work carried out by Despic et al. [15]. They performed linear sweep voltammetry and potential step investigations to determine the current–potential behaviour during copper and zinc co-deposition at a rotating disc electrode from a pyrophosphate–oxalate electrolyte where copper and zinc are bound to pyrophosphate and oxalate ligands, respectively. Although their solution was complex, containing sodium pyrophosphate, oxalic acid, sodium carbonate, sodium hydroxide, boric acid, and copper and zinc sulphates, some general conclusions can be drawn from their work. Their results indicate that pyrophosphate ions are adsorbed on the electrode surface prior to copper deposition, as was proposed by Konno and Nagayama [12]. In addition, they found that in the presence of zinc in the electrolyte, copper was discharged at lower overpotentials. They suggest that this is due to a decrease in pyrophosphate adsorption in the presence of zinc. They also computed the current efficiency for copper by integrating the charge for the anodic and cathodic sweeps in the potential region where only copper is plated and dissolved. The charge consumed in the dissolution process was 50% of that consumed during the deposition cycle; this led them to conclude that copper dissolved as Cu(I). Notably, this result is based on an assumption that current efficiency during copper reduction is 100%. Current efficiency for zinc deposition, on the other hand, was found to be low, about 10%. Current efficiency for Cu–Zn deposition, however, was not reported.

Clearly, current efficiency data on brass deposition from pyrophosphate electrolytes is incomplete and confusing. Since current efficiency has major implications on feasibility of alloy deposition as well as the range of alloy composition that can be obtained, it is important to fill this gap in our knowledge. In this work we have carried out a systematic investigation on current efficiency during brass deposition from a pyrophosphate electrolyte. Cu, Zn and Cu–Zn have been plated at a rotating disk electrode (RDE), a rotating cylinder electrode (RCE), and a quartz crystal microbalance (QCM). Whilst an RDE or RCE allows easy control of hydrodynamics, a QCM enables measurement of current efficiency in situ. Potentiostatic as well as potenti-

dynamic data have been collected during the deposition of individual metals and their alloy. Current efficiency has been found by integrating the current from linear sweep and gravimetric measurements. Alloy composition has been determined by carrying out energy dispersive X-ray analysis (EDX). Adsorbed species on the cathode surface, as well as current efficiency of metal and alloy deposition have been determined in situ by using the QCM.

2. Experimental

Electrolytes were prepared from reagent grade chemicals supplied by Aldrich. Zinc pyrophosphate, which is not commercially available, was prepared by precipitation of a saturated solution of zinc sulphate and potassium pyrophosphate. The resulting zinc pyrophosphate was filtered and dried in an oven at 110°C for over 24 h. All solutions were made of ultra pure water (> 10 M Ω purity). Three separate solutions were prepared to carry out Cu, Zn, and Cu–Zn deposition. Copper deposition was carried out from a solution composed of 0.01 M Cu₂P₂O₇, 0.37 M K₄P₂O₇ and 0.12 M KNO₃. The solution for electrodepositing zinc contained 0.09 M Zn₂P₂O₇, 0.21 M K₄P₂O₇ and 0.12 M KNO₃. The electrolyte used for alloy plating was composed of 0.01 M Cu₂P₂O₇, 0.09 M Zn₂P₂O₇, 0.23 M K₄P₂O₇, and 0.12 M KNO₃. In the following sections, these electrolytes are called copper plating, zinc plating and brass/alloy

plating solutions, respectively. The pH was adjusted to 8.4 for all solutions using pyrophosphoric acid. This metal to pyrophosphate ratio is identical to that suggested by Sree and Rama Char [6] so that we can compare our results directly with their findings.

Cyclic and linear sweep voltammetry experiments at a rotating disc electrode were carried out by a Versastat potentiostat controlled by personal computer with Voltmaster software. The rotating disc was supplied by Radiometer Copenhagen. It was placed in a cell supplied by the same company. The working electrode was a 2 mm diameter gold disc. The counter electrode was a platinum wire, and a standard calomel electrode (SCE), placed at a distance of 2 mm from the tip of the RDE, served as reference. Potential data were corrected for IR drop in the solution.

Potentiostatic metal deposition at a rotating cylinder was carried out by a Scanning Ministat supplied by Sycopel Scientific. The RCE was 6 cm long and 1 cm in diameter. The cylinder was made of steel. The steel cylinder was polished in a lathe to 2400 grit sand paper and then polished by diamond paste. Since brass does not nucleate on steel, a 10 μ m thick copper layer was then plated on the cylinder from an electrolyte containing 0.1 M copper pyrophosphate. This was done immediately before each plating experiment in order to avoid any oxide formation. The anode was a Pt-coated titanium mesh concentric cylinder placed at a distance of 3 cm from the cathode. The reference electrode was connected to a luggin placed 2 mm from the surface of the cathode.

Two different electrochemical quartz crystal microbalances have been used in this study. The QCM at Newcastle was a commercial Seiko QCA 917 (supplied by EG & G) while the other was manufactured at the University of Aarhus. The latter used a Hewlett Packard 53131A frequency counter. The EG & G QCA used 10 MHz AT-quartz crystals. The home made QCM employed 5 MHz AT-cut quartz crystals. Both sets of crystals were sputtered with gold, which formed the substrate material for metal deposition. The surface area available for metal deposition was 0.1 and 0.38 cm² at Newcastle and Aarhus, respectively. The frequency of the sputtered quartz crystals were found to be 8.5 MHz and 4.9 MHz for the EG & G and home made QCMs, respectively, when they were placed in distilled water. The frequency of the crystal during metal deposition was monitored visually on the oscillator; frequency readings were stored every 0.1 s.

Fig. 1 shows the electrochemical cells used in quartz crystal experiments. The quartz crystal, which was the working electrode, was kept vertical in all experiments, because this position produced a stable and reproducible frequency. The working electrode was conditioned by cycling the potential between 1.3 and –0.3 V versus SCE in a solution containing 0.23 M K₄P₂O₇

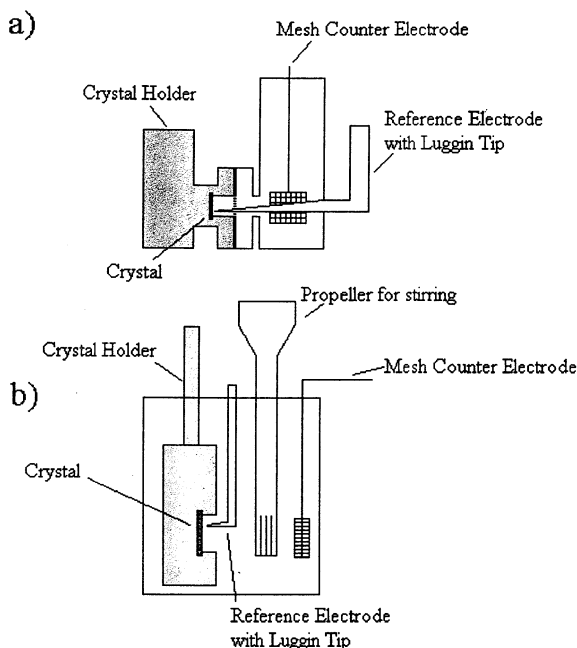


Fig. 1. Quartz crystal microbalance apparatus used in (a) Newcastle and (b) Aarhus.

before each experiment. The anode was a platinum mesh placed in the bulk solution and the reference was an SCE or a saturated mercury sulphate electrode (SMSE). It should be noted that in the Section 3 all potentials are referred to the SCE, with the difference in potential between SCE and SMSE being 0.40V [16]. The reference electrode was placed at a distance of 2 mm from the cathode surface at the University of Newcastle. In Aarhus, the reference was placed at a distance of 4–5 mm. In all QCM experiments the solution conductivity was high (0.1 Ω) and the total current did not exceed 20 mA. The resulting ohmic drop in solution is no more than 2 mV and therefore potential data were not compensated for IR losses.

3. Results

3.1. Rotating disc experiments

Polarisation data for Cu and Zn electroreduction at a rotating disc electrode is presented in Fig. 2. The rotation speed of the RDE is 1000 rpm and the scan rate is 0.30 V s⁻¹. The electrode potential is cycled from 0.20 V downwards and back. For the case of copper reduction, the lower limit of the scan is -1.1 V, whereas for the zinc deposition it is -1.5 V. A cathodic current for copper is observed when the electrode potential reaches below -0.8 V. As the potential is swept to more negative values, the current increases. The reverse scan exhibits hysteresis, with the reversible potential shifting towards -0.7 V. A dissolution peak with a shoulder is observed at potentials greater than -0.4 V. A cathodic current is observed with the zinc deposition electrolyte at -1.2 V and dissolution peak is observed at -1.3 V. A comparison of charge consumed during the anodic and cathodic part of the potential sweep for copper and zinc discharge showed that less than 10% of the reduced species were oxidised. This suggests that hydrogen discharge consumed a significant portion of the current during cathodic polarisation of copper and zinc electrodeposition. A visual inspection of the electrode showed that some amount of deposit remained on the surface at the end of a voltammetry experiment.

Partial currents for copper and zinc discharge can be computed from the polarisation data if the current for hydrogen evolution is known. In an attempt to determine the current for hydrogen evolution, cyclic voltammetry was carried out with a solution containing 0.23 M K₄P₂O₇ and 0.12 M KNO₃. It was found that the reduction current was 'higher' when copper and zinc pyrophosphate are absent from the electrolyte, possibly because the metal ion complexes inhibit hydrogen evolution by adsorbing on the electrode surface. This means that the partial current for copper and zinc cannot be calculated from RDE polarisation data.

3.2. Rotating cylinder experiments

Cyclic voltammetry experiments were then carried out at a rotating cylinder electrode to verify the current-potential data obtained at the RDE. The rotation speed was set to 1000 rpm, and a scan rate of 0.30 V s⁻¹ was used. Although visual observation confirmed that copper and zinc were plated at the cylinder, it was not possible to dissolve the deposits by sweeping the potential anodically. On the application of positive overpotentials a blue-green film was formed on the copper and a grey film was formed on zinc, which blocked further dissolution. Both RDE and RCE results indicate that current efficiency obtained from cyclic voltammetry is inaccurate.

A gravimetric technique was then employed to determine the current efficiency. Copper and zinc were plated on to the RCE at a particular potential. The current efficiency was measured by comparing the charge passed during an experiment and that calculated by measuring the change in the weight of the cylinder due to the deposited metal using Faraday's law. The current efficiency for copper and zinc deposition are very low near the reversible potential; it was, therefore, difficult to determine the current of copper and zinc accurately near these potentials. We have presented current efficiency data that could be measured accurately.

Fig. 3(a) shows the current efficiency for copper and zinc deposition. The efficiency for copper discharge is small at low and high overpotentials, and passes through a maximum of 45%. Current efficiency for zinc is below 10% at all potentials. Current-potential data for copper and zinc were computed using the current efficiency and the applied current density. These data are presented in Fig. 3(b). As illustrated in the figure, copper reduction commences at -0.8 V. A current plateau, similar to a mass transfer limiting current, is observed at potentials below -1.0 V. For a rotation speed of 1000 rpm, a metal ion concentration of 0.01 M, and a diffusion coefficient of 7.2×10^{-6} cm² s⁻¹ the diffusion limiting current is calculated to be 10.8 mA cm⁻² [17]. The current plateau is somewhat higher than this value (and rises slightly with increasing potential), presumably due to an increase in agitation due to hydrogen evolution. Zinc deposition occurs only at potentials below -1.5 V. Although zinc concentration is nine times higher than that of copper, a high zinc deposition current cannot be attained due to co-evolution of hydrogen. In fact, at high negative overpotentials, non-metallic, dark deposits were obtained.

Partial currents for copper and zinc during brass plating were then calculated by co-depositing the two metals from a brass plating solution. Brass was plated at a constant potential, and the amount of metal deposited was determined from weight measurements.

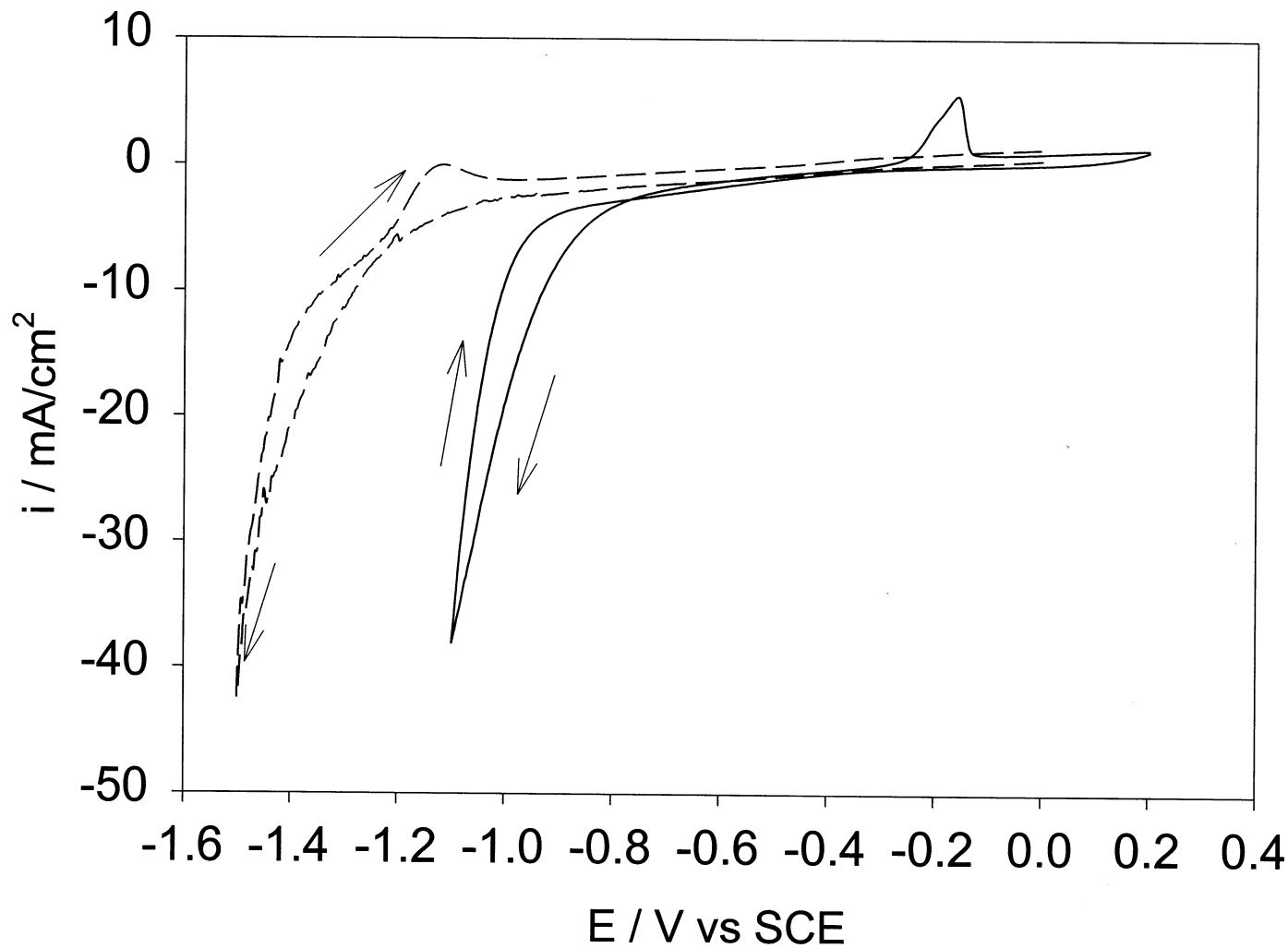


Fig. 2. Cyclic voltammogram for copper reduction from a Cu electrolyte and Zn reduction from copper and zinc plating solutions. Disc rotation speed 1000 rpm. — copper; - - - - zinc.

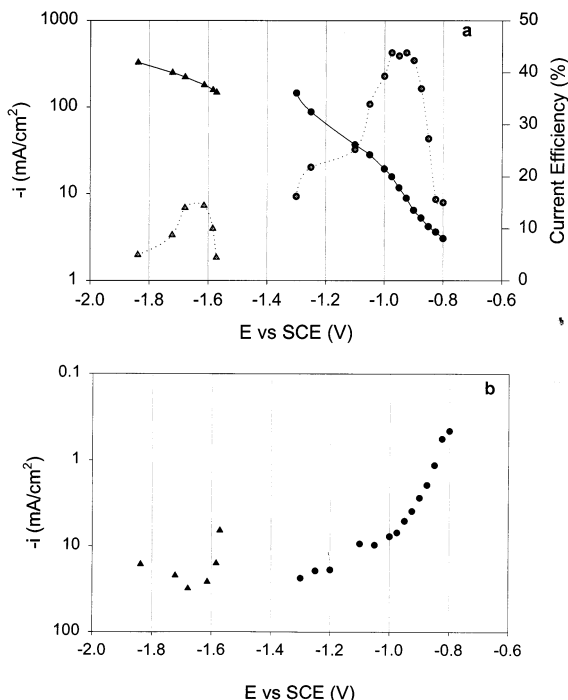


Fig. 3. (a) Current efficiency and total measured current for copper and zinc reduction from copper and zinc plating solutions. (b) Partial currents for copper and zinc at different potentials at a RCE as obtained from gravimetric measurements. ●, copper; ▲, zinc.

The composition of the deposit was determined by EDX using an Oxford Link ISIS II with a 4 nm diameter probe. The weight of each metal was computed from gravimetry and alloy composition. Faraday's Law was used to calculate the charge consumed during the discharge of each metal. It should be mentioned that the content of oxygen, phosphorus and

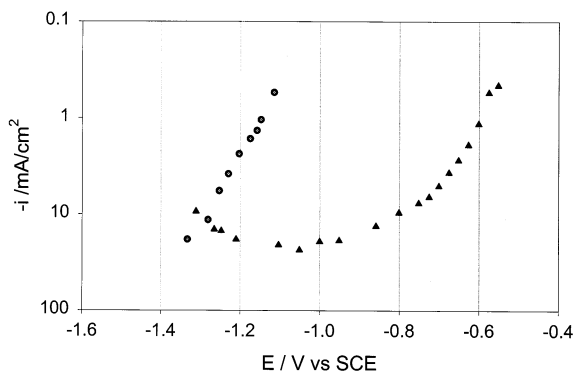


Fig. 4. Partial current densities for copper and zinc reduction during brass deposition from a pyrophosphate electrolyte as determined from gravimetric measurements and EDAX. ▲, copper; ●, zinc.

nitrogen in the deposit was within the background signal in an EDX analysis. The plated brass, therefore, was considered to be metallic. In addition, islands of only copper or zinc were not detected, which suggests that the alloy was a solid solution.

The partial currents for copper and zinc, as calculated from these measurements, are presented in Fig. 4. Copper reduction commences at -0.5 V during brass plating, which is much higher than that observed for copper deposition. A current plateau of a magnitude similar to the mass transfer limiting current for Cu(II) is observed beyond -0.8 V. Zinc reduction commences at potentials below -1.2 V, higher than that observed during electrodeposition from a zinc plating solution. This shows that brass deposition is feasible at potentials below -1.2 V, although the plating efficiency is low, i.e. between 22 and 15%. In order to determine if current efficiency changed as the deposit got thicker (i.e. varied with time), brass foils of thickness ranging between 5 and 30 μm were plated. The current efficiency was found to remain unchanged.

The important difference between the deposition characteristics of individual metals (copper and zinc) and their alloy is a shift in the reversible potential for copper and zinc to more positive values during brass plating. Konno and Nagayama [12] and Despici et al. [15] have reported such a shift during copper deposition from pyrophosphate. Konno and Nagayama [12] suggested that the shift is due to the fact that pyrophosphate cannot adsorb on the surface when copper concentration in the solution is high, and Despici and co-workers [15] surmised that it may be because zinc complexes with pyrophosphate which lowers the pyrophosphate concentration in solution. Our results show that pyrophosphate adsorption as well as hydrogen evolution are inhibited when Cu(II) and Zn(II) are present in the electrolyte, thereby enabling brass deposition.

3.3. Quartz crystal microbalance experiments

Before metal and alloy deposition experiments could be performed, a series of calibration measurements for the QCM had to be undertaken. The oscillation frequency of a QCM in a shearing fluid is expected to decrease by the following [18]

$$\Delta f_L = \left(\frac{\eta_L d_L}{\pi \mu_Q d_Q} \right)^{1/2} f_{\text{air}}^{3/2} \quad (1)$$

When metal is deposited from an electrolyte on to the quartz crystal, there is a corresponding to a decrease in frequency according to the Sauerbrey equation [19]:

$$-\Delta f = C f_L^2 \Delta m \quad (2)$$

where $f_L = f_{\text{air}} - \Delta f_L$. Since C and f_L are related to the physical properties of the crystal substrate and the electrolyte, the equation reduces to

$$\Delta f = \alpha \Delta m \quad (3)$$

where α can be derived experimentally by depositing a metal on the crystal at 100% current efficiency.

Once α is known for a QCM, mass changes due to adsorption, electro-deposition or dissolution, and the formation of viscous layers on the electrode surface can be detected by measuring changes in frequency and combining it with the Faraday equation to give a 'current' corresponding to the mass change

$$i_{\text{calc}} = \alpha \frac{M}{zF} \frac{\delta f}{\delta t} \quad (4)$$

In Eq. (4), i_{calc} is the calculated current, δt is the time duration, M the atomic mass of the metal (or the average mass in the case of an alloy), z the number of electrons exchanged in the reaction, and F Faraday's constant. When a frequency change is solely due to the change in mass of the crystal due to electrodeposited metal (or alloy), i_{calc} has to equal the deposition current of the metal or alloy. If, however, frequency changes arise from other sources, i.e. adsorption of species on the surface, these will also result in a signal for i_{calc} without the passage of a faradaic current. By comparing the value of i_{calc} with the faradaic current one can determine whether the mass change of the QCM is due to an electron transfer process. Throughout this paper, i_{calc} is the current calculated from mass changes of the crystal; it should not be confused (or equated) with the measured faradaic current.

The first calibration measurement was carried out to determine the value of α . Copper was deposited on the QCM at -0.1 V using a solution of 0.1 M CuSO_4 in 0.5 M H_2SO_4 . Since copper reduction occurs with a current efficiency of 100% at these potentials, this has been adopted as a standard method to calibrate QCMs [20,21]. In order to avoid sharp changes in i caused by sudden changes in $\Delta f/\Delta t$, an average of 5 points were used to calculate i from Eq. (4) in our experiments. The calibration measurement showed that Eq. (4) was valid up to 1.7% of f_L , which corresponded to a mass change of $1500 \mu\text{g cm}^{-2}$. The frequency changes during copper, zinc and brass plating experiments were much lower, and therefore Eq. (4) was valid in all our experiments. A typical value for α is $1.39 \times 10^8 \text{ Hz g}^{-1}$ with a standard deviation of only $0.01 \times 10^8 \text{ Hz g}^{-1}$. This is slightly lower than the theoretical value of $1.49 \times 10^8 \text{ Hz g}^{-1}$ predicted by the Sauerbrey equation for copper deposition [18,19] due to the roughness of the gold substrate.

A second calibration measurement was performed to determine if i_{calc} followed the measured faradaic current during cyclic voltammetry. Here, copper was plated and dissolved by scanning the electrode potential between 0.50 and -0.30 V. It was found that the i_{calc} followed closely the measured current with only one exception: a

change in frequency was observed around -0.03 V due to adsorption and desorption of sulphate ions.

In order to compare mass transfer conditions at the QCM with those at the RCE, a the limiting diffusion current for copper deposition from the 0.1 M $\text{CuSO}_4/0.5$ M H_2SO_4 solution was also measured. In these experiments copper was plated for 300 s at different potentials and the mass change was calculated from the frequency change of the crystal. It was found that the limiting current of copper was 11.7 mA cm^{-2} ; this means that the diffusion limiting current for 0.01 M CuSO_4 (which is the concentration used in the copper and brass plating solutions) should be 1.17 mA cm^{-2} , nine times lower than that at an RCE.

Following the calibration procedure, a cyclic voltammetry scan between 0.50 and -1.50 V was performed with a 0.23 M $\text{K}_4\text{P}_2\text{O}_7$ and 0.12 M KNO_3 solution to determine the potential region where pyrophosphate ions adsorb. The results from this experiment are shown in Fig. 5. The small arrows in the figure indicate the direction of the scan. The measured current is the solid line, frequency changes are the dashed line, and the dotted line shows i_{calc} . As shown in the figure, no current is measured until -1.1 V, where hydrogen evolution begins. Frequency changes show other phenomena on the electrode surface: (1) there is a slight decrease in frequency at -0.65 V (where no current is measured) and an increase in frequency around -1.0 V, just before hydrogen evolution commences, (2) a decrease in frequency is observed beyond -1.4 V, a region where there is significant hydrogen evolution. The first decrease in frequency is attributed to an adsorption of non-electro-reactive species on the surface, a pyrophosphate species [12]. These species begin to desorb at -1.0 V, which results in an increase in frequency. It can be seen that the adsorption and desorption of pyrophosphate ions shows up as a peak in the i_{calc} curve. The noisy decrease in frequency beyond -1.4 V is due to formation and discharge of gas bubbles on the electrode surface. However, there is an overall decrease in the QCM frequency of about 300 Hz during the potential cycle. This overall frequency change is caused by the vigorous hydrogen evolution, due to attached bubbles or formation of precipitates.

A cyclic voltammetry scan at a QCM for a copper plating solution is presented in Fig. 6. The solid line, which denotes the measured current, shows that an electroreduction of copper begins at potentials close to -0.8 V, as was found in the RCE and RDE experiments. There is a hysteresis in the reverse scan, and the reduction current is zero at -0.9 V. An anodic current is observed when the potential exceeds -0.4 V where two anodic peaks for copper dissolution is observed. The deposit is dissolved completely by the time the potential reaches 0.4 V.

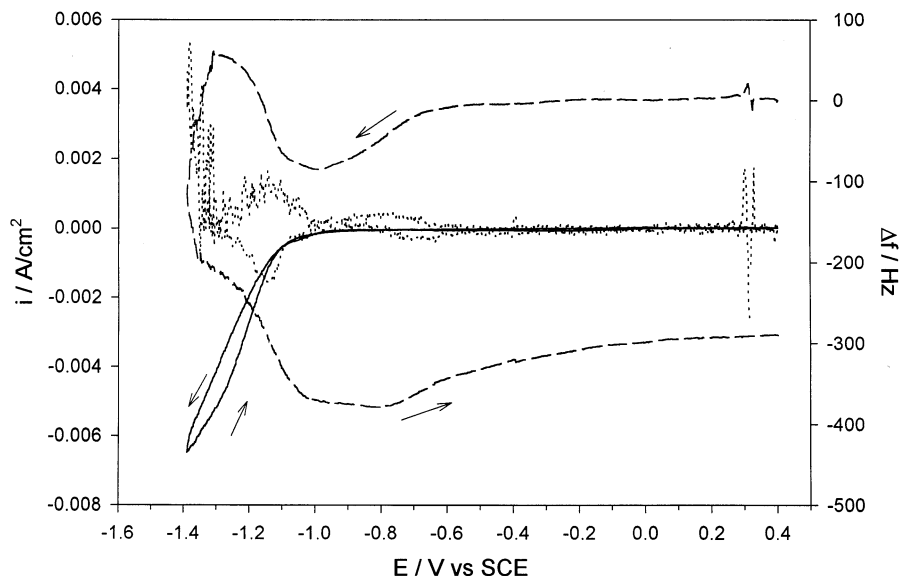


Fig. 5. Cyclic voltammogram of the supporting electrolyte with scan rate 0.02 V s^{-1} showing the measured current (—), calculated current i_{calc} (.....) and frequency change (----).

Frequency changes at the QCM in Fig. 6 impart more information on processes occurring at the electrode. In the outward scan there are two clear separate regions where there is a decrease in frequency. The first region starts at -0.65 V where the measured current is zero, corresponding to pyrophosphate adsorption. A faster change in frequency is observed below -0.75 V . It lasts until -0.92 V . The second region lies between

-0.92 and -1.05 V . Here again there is a slow decrease in frequency between -0.92 and -1.05 V . Beyond these potentials there is a monotonic decrease in frequency as more and more copper continues to deposit. When the potential is reversed, copper continues to plate until -1.05 V . A slow increase in frequency is observed after that, it lasts until -0.4 V after which a steady increase in frequency is observed due to

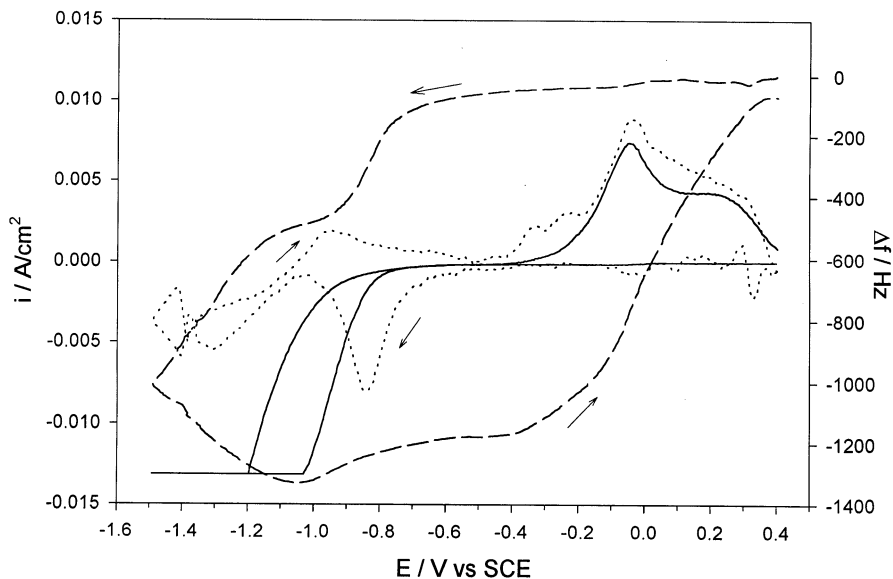


Fig. 6. Cyclic voltammogram of the copper plating solution with scan rate $= 0.03 \text{ V s}^{-1}$. Measured current —, calculated current i_{calc} and frequency change ----.

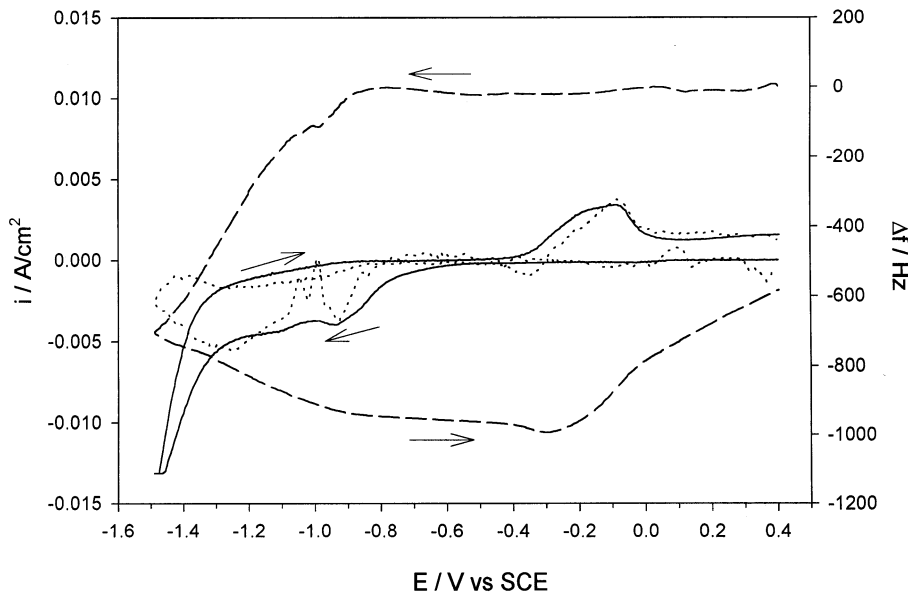


Fig. 7. Cyclic voltammogram of the brass plating solution with a scan rate of 0.05 V s^{-1} showing the measured current —, calculated current i_{calc} and frequency change ----.

copper dissolution. Frequency changes show that pyrophosphate ions are adsorbed between -0.65 and -1.05 V . Two different kinds of copper are deposited on the QCM: (1) one which is reduced at potentials below -0.75 V and (2) another which is deposited at potentials below -1.05 V . From frequency changes and Eq. (3) it is calculated that the first layer consists of approximately 30 mono-layers. This is also observed in the reverse scan where two separate peaks for copper dissolution are observed.

The dotted curve, which represents i_{calc} shows some interesting aspects: (1) that the peak at $\approx -0.85 \text{ V}$ is bigger and sharper than that observed at -0.9 V in the reverse scan, (2) the measured currents are much bigger than those calculated from frequency changes during the deposition cycle, (3) that there are two peaks for copper deposition and dissolution, and (4) that the measured and calculated anodic current at potentials greater than -0.4 V are in good agreement. The first aspect shows that when there are two processes occurring at the electrode surface, i.e. copper deposition and pyrophosphate adsorption, which are additive between -0.65 to -1.05 V , a single, strong peak may be observed. In the reverse scan, where only pyrophosphate desorbs, a weaker peak (within the same potential regime) is obtained. The second aspect shows that the current efficiency for metal deposition is low. The third observation shows that the copper deposited on the gold exhibits different electrochemical and thermodynamic behaviour from copper depositing on copper. The fourth aspect shows that since the measured and calculated currents for copper dissolution are in close

agreement, and i_{calc} is computed with $z=2$, copper dissolves as Cu(II) species.

Although an attempt was made to carry out zinc deposition from a $\text{Zn}_2\text{P}_2\text{O}_7/\text{K}_4\text{P}_2\text{O}_7/\text{KNO}_3$ solution, zinc deposits could not be obtained because of excessive hydrogen evolution (which produced frequency oscillations in the QCM). In addition, the gold layer was often stripped from the QCM by gas bubbles which stops further metal deposition. These results are in agreement with the RCE results where zinc was plated at very low current efficiency (cf. Fig. 3).

A cyclic voltammogram for brass deposition is depicted in Fig. 7. The measured current shows that copper deposition commences below -0.6 V , as was observed in the RCE experiments. Two minor current peaks are observed at -0.92 and -1.1 V on the forward scan followed by a dominant current attributed mainly to hydrogen evolution. On the reverse scan, the reduction currents are found to be lower. A broad dissolution peak is observed beyond -0.4 V , where copper dissolution is expected. Although brass is expected to dissolve at less noble potentials, a layer of copper covers the deposited brass (plated during the reverse scan) and prevents brass from dissolving. Interestingly, the dissolution current is maintained beyond -0.4 V , possibly due to the slow oxidation of brass.

A comparison of i_{calc} and measured current reveals more details regarding brass deposition. It is striking that there is no significant pyrophosphate adsorption between -0.65 and -1.05 V . This shows that the presence of zinc ions in the solution inhibits pyrophosphate ion adsorption. Two peaks for i_{calc} are detected at

potentials of -0.9 and -1.2 V. As before, this shows that two different kinds of copper are deposited. From frequency changes it is found that the initial layer consists of approximately ten monolayers of copper. At potentials more negative than -1.2 V as well as the remaining forward scan, calculated values of deposition current remain much lower than the measured current. Frequency changes due to metal deposition in the reverse scan are also smaller. These data show that although copper deposition occurs at a reasonable current efficiency, it drops when brass is deposited. A decrease in mass of the QCM begins at -0.32 V, showing copper dissolution. Fair agreement between measured copper oxidation currents and i_{calc} show that Cu dissolves as Cu(II) species. It must be mentioned that the deposit continued to dissolve after the scan was terminated (the potential was held at 0.4 V) and the frequency returned to the initial value after 15 s showing that the deposit was completely dissolved.

Thereafter, a set of potentiostatic experiments was carried out to determine the current efficiency during brass deposition. Brass was plated for 300 s at a particular potential on the crystal and the current efficiency and partial current was determined from frequency changes, the measured current, and the alloy composition as measured by EDX. Fig. 8 shows the current efficiency and composition of brass at different potentials. As was found in the RCE experiments, the current efficiency decreased from 30 to 5% as the potential was lowered and the alloy became more zinc-rich. Oxygen and phosphorus were not detected in the EDX analysis showing that the deposits were metallic.

4. Discussion

Our experimental results show that it is difficult to measure current efficiency during brass deposition from a pyrophosphate electrolyte because the current efficiency is low. Cyclic voltammetry and anodic stripping are difficult to implement and interpret because current efficiency changes with applied potential. In addition, the stripped metal forms an anodic film which prevents further dissolution of the metal. Gravimetric techniques are suitable, but one has to be careful that non-metallic components are not incorporated in the deposit. However, it is clear that since brass is plated at potentials where substantial hydrogen evolution occurs (especially for Zn-rich alloys), it is not possible to plate this alloy at a high current efficiency. Under no condition was our current efficiency comparable to those claimed by Rama Char and coworkers [5–7]. Although we carried out plating experiments at room temperature, and they reported results for deposition experiments carried out at 40°C , an increase in temperature should increase all electrochemical reactions and therefore the change in current efficiency should not be disproportionate. In this regard our results corroborate the current efficiencies found by researchers in references [8–11].

The QCM measurements also provide some insight into the electrodeposition process. For example, when there are no metal salts in the electrolyte, pyrophosphate is adsorbed on the electrode surface and hydrogen evolution is the highest. On the addition of copper pyrophosphate, pyrophosphate is adsorbed more strongly and the hydrogen evolution current decreases. This shows that there is competitive adsorption be-

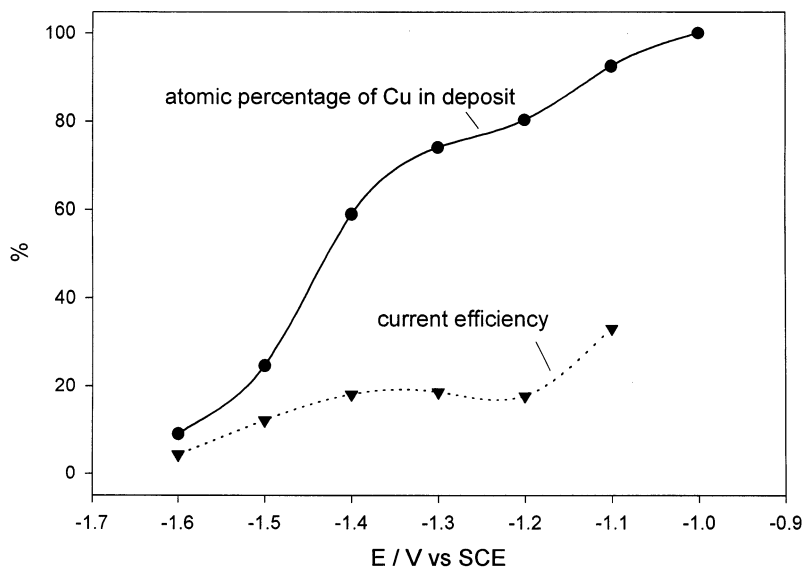


Fig. 8. Copper content and current efficiency of during potentiostatic deposition of brass from the brass plating solution.

tween the (pyrophosphate) species participating in the discharge of hydrogen and copper. On the addition of zinc pyrophosphate, the adsorption of pyrophosphate is blocked altogether. Researchers have suggested that pyrophosphate adsorption on the electrode is diminished in presence of zinc due to strong ligation with zinc atoms [15]. The decrease in pyrophosphate adsorption results in copper and zinc reduction at less noble potentials. Despic et al. have called it a catalytic effect of zinc during copper deposition [15]; however, it is the competitive adsorption of pyrophosphate species leading to hydrogen, copper, and zinc discharge which governs the electrode reaction.

The QCM experiments support the kinetic model for copper deposition proposed by Konno and Nagayama [12]. These researchers found that there were two different Tafel slopes during copper reduction from a pyrophosphate electrolyte. They proposed that copper reduction showed a higher Tafel slope at low overpotentials because pyrophosphate species were adsorbed on the electrode. At higher overpotentials the Tafel slope was smaller because pyrophosphate species were not present. This model was indirectly corroborated by Despic et al. [15] who noted two dissolution peaks during cyclic voltammetry experiments. Our QCM experiments provide more direct evidence which show that copper is discharged in the presence and absence of adsorbed pyrophosphate species at low and high overpotentials, respectively.

The current efficiency results bring into question a few interpretations regarding copper deposition and dissolution reported previously. For example, Despic et al. showed that copper dissolved as a Cu(I) species in a pyrophosphate–oxalate electrolyte. Their calculations are based on an assumption that copper reduction occurs at 100% current efficiency. However, we found that copper deposition is characterised by a current efficiency of 40–50%. Therefore, when the metal is stripped anodically, the amount of metal dissolved will be only 50% compared to that if the current efficiency were 100%. Since copper can dissolve in Cu(I) or Cu(II) forms, this may be construed as copper oxidising to its cuprous form. However, the simultaneous measurement of faradaic current and frequency changes show conclusively that copper dissolves as Cu(II) in a pyrophosphate electrolyte. It is unclear if this is also true for a pyrophosphate–oxalate electrolyte.

This investigation shows the importance and potential of using QCM for investigation regarding metal and alloy deposition. Current–potential data from cyclic voltammograms at an RDE are difficult to interpret when side reactions such as hydrogen evolution or oxide film formation occurs. In addition, deposits from an RDE are often not amenable to surface analysis and characterisation, which limits the calculation of partial current data. An RCE is more useful in determining

partial current as well as deposit characterisation. However, neither an RDE or and RCE are useful for the detection of adsorbed species or following in situ the different processes occurring the electrode. A QCM is useful to collect such information, although it must be kept in mind that it lacks mass transfer regulation. Recently a quartz crystal micro-balance fitted at the tip of a rotating disc has been used for colloid deposition [22], Cu–Se plating [23] and gold leaching [24]; clearly the use of this tool will be useful to study the deposition of alloys such as brass.

5. Conclusion

In this study a rotating disc electrode, a rotating cylinder electrode, and a quartz crystal microbalance were used to systematically investigate the current efficiency during the deposition of copper, zinc, and brass from a pyrophosphate electrolyte. Current efficiency measurements at the RDE and RCE proved difficult, since it was often not possible to strip completely the deposit off the electrode in the anodic sweep of the cyclic voltammogram. Hence gravimetry was used to determine current efficiency at the RDE and RCE. The QCM was used to determine the current efficiency in situ. It was found that the current efficiency for copper, zinc as well as brass are well below 100%, in contrast to those reported by Rama Char and co-workers [5–7].

Partial current densities for copper and zinc during brass deposition at an RCE were measured using gravimetry and EDX measurements. It was found that copper and zinc are discharged at more noble potentials during brass deposition as compared to that observed for individual metal deposition. QCM measurements showed that pyrophosphate adsorption is significant when copper is plated from a pyrophosphate solution containing copper ions, but is inhibited when zinc ions are added to the electrolyte. It was found that two different kinds of copper are plated from a pyrophosphate electrolyte: one in the presence and the other in the absence of adsorbed pyrophosphate. Simultaneous measurement of faradaic current and frequency changes of the QCM showed that copper dissolves entirely as Cu(II) ions. It was concluded that the quartz crystal micro-balance is an important tool for measuring current efficiency in situ and examining adsorption effects during an electrodeposition process.

Acknowledgements

The authors would like to thank Professor D. Britz and Dr T.A. Green for useful discussion on several matters. This work was supported by a University Research Studentship from the University of New-

castle. EDX at Newcastle was carried out by the Materials Analysis Unit and by Prof. N. Pind and J.K. Christensen in Aarhus. The help of Sabine Bonhomme in some RCE experiments is also acknowledged.

References

- [1] F.A. Lowenheim, *Modern Electroplating*, Wiley, New York, 1974.
- [2] A. Brenner, *Electrodeposition of Alloys — Principles and Practice*, vol. I, Academic Press, London, 1963.
- [3] Vaid and T.L. Rama Char, *J. Sci. Ind. Res. (India)*, 15 B (1956) 509.
- [4] K. Thompson, M. de Kay, *Met. Chem. Eng.*, 10 (1912) 458–461.
- [5] T.L. Rama Char, *Electroplat. Met. Finish.* 10 (1957) 347–349.
- [6] V. Sree, T.L. Rama Char, *Electroplat. Met. Finish.* 12 (1959) 326–330.
- [7] T.L. Rama Char, *Electroplat. Met. Finish.* 12 (1959) 391–392.
- [8] M. Ishikawa, H. Enomoto, *New Mater. New Process.* 2 (1983) 243–251.
- [9] M. Ishikawa, H. Enomoto, M. Matsuoka, C. Iwakura, *Electrochim. Acta* 40 (1995) 1663–1668.
- [10] A.C. Hamilton, *Plat. Surf. Finish.* 81 (1995) 48–50.
- [11] M. Ishikawa, H. Enomoto, M. Matsuoka, C. Iwakura, *Electrochim. Acta* 39 (1994) 2153.
- [12] H. Konno, M. Nagayama, *Electrochim. Acta* 23 (1978) 1001.
- [13] H. Konno, M. Nagayama, *Electrochim. Acta* 22 (1977) 353.
- [14] T. Vagramyan, J.S.L. Leach, J.R. Moon, *Electrochim. Acta* 24 (1979) 231.
- [15] A. Despic, V. Marinovic, V.D. Jovic, *J. Electroanal. Chem.* 339 (1992) 473.
- [16] A.J. Bard, L.R. Faulkner, *Electrochemical Methods, Fundamentals and Methods*, Figure E-1, Wiley, New York, 1980.
- [17] M. Eisenberg, C.W. Tobias, C.R. Wilke, *J. Electrochem. Soc.* 101 (1954) 307.
- [18] S. Bruckenstein, M. Shay, *Electrochim. Acta* 30 (1985) 1295.
- [19] G. Sauerbrey, *Z. Phys.* 155 (1959) 206.
- [20] M. Zhou, N. Myung, X. Chen, K. Rajeshwar, *J. Electroanal. Chem.* 398 (1995) 5.
- [21] C. Klingenberg, MSc Thesis, University of Aarhus, May, 1999.
- [22] N. Shirtcliffe, *Colloids Surf. A* 155 (1999) 277.
- [23] A. Marlot, J. Vedel, *J. Electrochem. Soc.* 146 (1999) 177.
- [24] J. Zheng, I.M. Ritchie, S.R. La Brooy, P. Singh, *Hydrometallurgy* 39 (1995) 277.